Vitis Vinifera extract counteracts exposome aggressions in a 3D full-thickness human skin model exposed to different environmental stressors

Zhuo Cai[1], Yuan Lu[1], Marion ALBOUY[2], Sandrine HERAUD[2], Amélie THEPOT[2], Bingjie Wang[1], Morgan DOS SANTOS[2]

1. Guangzhou Yatsen Global Co., Ltd. 510030 Guangzhou, China
2. LABSKIN CREATIONS, Edouard Herriot Hospital, 69003 LYON, France

Abstract

The skin barrier protects the body from a variety of environmental stresses and the accumulations of aggressions on the skin will lead to impairment of skin barrier function and speed up skin aging. To protect the skin from numerous pollutants and daily stresses, we developed an innovative Vitis Vinifera Extract and its effects on epidermal barrier and cohesion, dermal extracellular matrix synthesis and anti-oxidant were studied.

To validate the potential repairing properties of V. vinifera extract, a 3D full-thickness human skin model was developed, along with exposure to individual daily stresses including environmental pollutants, UVA and UVB radiations, and detergent.

All environmental stresses individually applied to our 3D skin model significantly affected both cellular and tissular functionalities. Comparatively to the unstressed control condition, our results demonstrated a significant increase in MMP-1, NQO1, and metallothionein expression and a decrease in type I collagen, filaggrin, claudin-1, ceramides, and LCE-1A expression, in our 3D skin model either exposed to UVA and UVB radiations, urban dust or SDS.

In conclusion, the application of V. vinifera significantly counteracts the effects of exposome aggressions in an in vitro skin model, suggesting its protective effects against daily UV and pollutant exposure.

Keywords: V. vinifera, exposome, pollution, 3D skin model

1. Introduction

The skin is an essential barrier, protecting the body against the environment and its numerous pollutants and daily stresses [1]. Several exposome aggressions, such as sunlight and pollution are known to affect the skin and can trigger molecular processes that accelerate premature skin aging through mechanisms including oxidative stress, inflammation, and impairment of skin functions. Self-induced factors such as diet, smoking and other miscellaneous factors, including lifestyle choices and use of cosmetic products, also play a significant role in potentiating skin aging [2].

Natural products such as plant extracts have been involved in the skin anti-oxidant and anti-aging cellular protection against environmental stress [3]. *Vitis vinifera* regarded as an important medicinal plant and its main active polyphenol, resveratrol, have shown considerable antioxidant properties, besides possessing protective and therapeutic effects against various skin complications such as inflammation and wound healing [4].

In the present study, we aimed to study potential repairing properties conferred by *V. vinifera* extract in a 3D full-thickness human skin model exposed to individual stress including environmental pollutants, UVA and UVB radiations and detergent. In particular, we focused on the effect of the *V. vinifera* extract on epidermal barrier and cohesion, dermal extracellular matrix synthesis and anti-oxidant effects.

2. Material and Methods

2.1 Ethical considerations and human cells isolation

Adult skin was collected according to the Declaration of Helsinki Principles and its use was declared to the French Research Ministry (declaration n° DC-2020-4346). A written informed consent was obtained from the donor according to the French bioethical law of 2014 (loi 94–954 du 29 Juillet 1994). Primary cultures of human fibroblasts and keratinocytes were established from healthy skin biopsy obtained from adult patient (> 40 years old). Normal human epidermal keratinocytes (NHEK) and dermal fibroblasts (NHDF) were isolated from human skin as previously described [5].

2.2 Full-thickness human skin models engineering, stresses exposure and product treatment

3D full-thickness reconstructed skin model was obtained by culturing NHDF in a scaffold made of collagen, glycosaminoglycans and chitosan (LabSkin matriX®, Lyon, France) during 21 days under optimized cell culture conditions for ECM neo-synthesis as previously described [6]. NHEK were then seeded on the top of the dermal equivalent constructs and raised at the air/liquid interface to allow the formation of the epidermal compartment.

Different stresses were applied to the skin equivalent samples between day 42 to 45. Seven days after being raised to the air–liquid interface, skin substitutes were exposed to two consecutive doses of 100mJ/cm2 UVB and then 12J/cm2 UVA irradiations. Sodium Dodecyl Sulfate (SDS) 0.5% stress was performed during the last 3 hours of the tissue reconstruction at days 45. Pollution stress was applied at day 44 and let in contact with the culture medium during the last 24 hours of the tissue reconstruction. *Vitis vinifera* extract was added in the cell culture medium at 0.1% from day 35 to the end of the culture.

Skin equivalent samples harvested at day 45 of total cell culture were immediately fixed in neutral buffered formalin 4% for 24 h and embedded in paraffin or in OCT compound and frozen at −80°C, for histological and immunohistological analysis, respectively. For each cell culture condition and analysis, 3D skin equivalents were produced in triplicate.

2.3 Reagents and Antibodies

Vitis vinifera extract were surface-sterilized and were each cut into small pieces, wounded, and placed on solid medium. Cell suspension cultures of vitis vinifera were established from fruit callus and maintained under continuous fluorescent light (5000 lux) at 25±1°C in Erlenmeyer flasks containing cell suspension on an orbital shaker. The maintenance medium contained macro-elements, microelements and vitamins and was supplemented with sucrose, 1-naphtalene-acetic acid, and kinetin. Cells were sub-cultured every week by inoculating the cells at a 1/5 (v/v) ratio into fresh medium. The obtained cells were elicited and used for the different studies after extract preparation.

SDS and Urban dust were purchased from Sigma Aldrich and used according to manufacturer's instructions. Rabbit polyclonal anti-metallothionein, -NQO1, -LCE1A, type-I collagen and mouse monoclonal anti-filaggrin, claudin-1, -ceramides, -MMP1 antibodies were used for immunohistochemistry analysis.

2.4 Histological staining

Paraffin-embedded formalin-fixed samples were cut into 5 µm sections. After dewaxing and rehydration, sections were stained with haematoxylin, phloxin and saffron (HPS) for routine histological analysis.

2.5 Immunohistological analysis

For immunofluorescence on paraffin sections, after heat-mediated antigen retrieval treatment, tissue sections were incubated in 5% H_2O_2/3% bovine serum albumin to inactivate endogenous peroxidases. Non-specific binding was blocked in PBS containing 5% of BSA. Sections were then incubated with primary antibodies diluted in PBS/BSA 5% overnight at room temperature. After incubation for 1 hour with the peroxidase labelled polymer conjugated to secondary antibody, the antigen was detected with 3,3-diaminobenzidine tetrachloride (Dakocytomation) as the substrate. Tissue sections were subsequently counterstained using Harris' hematoxylin (25%, Sigma Aldrich). As negative control, the corresponding IgG class replaced primary antibody.

For immunofluorescence on OCT-fixed slices, labeling was performed on air-dried 5 µm cryosections and incubated with primary antibodies. Secondary AlexaFluor-488- or Alexa-568-conjugated anti-mouse or anti-rabbit antibodies (Molecular Probes, Invitrogen) were incubated 1 h at room temperature. Nuclear counterstaining using DAPI was carried out routinely. As a negative control, primary antibody was replaced by the corresponding IgG class.

2.6 Image acquisition and analysis

Specimens stained in HPS were observed using an Axioskop 2 Plus optical microscope (Zeiss), and images were captured using DS-Ri1 CCD camera (Nikon) and NIS-Elements software (Nikon). Sixteen-bit images were saved in an uncompressed tagged image file format (tiff). Nine representative images were captured for each condition in the same manner.

Image processing and analysis were performed using the software ImageJ (Rasband, W.S., ImageJ, U. S. National Institutes of Health, Bethesda, Maryland, USA, http://imagej.nih.gov/ij/, 1997-2017).

For immunohistochemical staining, positively stained-tissue areas were automatically detected and segmented from other pixels. Images were then converted in binary images, treated by mathematical morphology and sieved for isolating the regions of interest. The surface area of interest was measured automatically. For immunofluorescent staining, images were first converted to RGB images and then deconvolved into their red, blue and green components. The red component was identified as the biological target.

Depending on the biological target, positively stained-tissue areas were normalized by total dermal or epidermal area (results expressed in percentage of density) or normalized by epidermal dermal junction length.

2.7 Statistical Analysis

All data are presented as mean values ± standard deviations. Statistical significance in the data was assessed running Student's t-test. Each set of data relates to a comparison *versus* untreated control. Statistical significant differences are indicated by asterisks as follows: *P < 0.05, **P < 0.01 and ***P < 0.001.

3. Experimental results

3.1 Vitis viniferas protects from UVA+UVB cutaneous alterations in a 3D full-thickness reconstructed skin model

To assess the efficiency of *Vitis Vinifera* extract in protecting skin against photodamages induced by UV radiations, we first developed a full-thickness 3D adult human skin equivalent comprising a differentiated epidermis and a living dermal equivalent exposed to both UV_A and UV_B radiations. As can be seen in Fig. 1, reconstructed human skin *in vitro* presented the main skin characteristic features, including a pluristratified epithelium covered by a well-developed *stratum corneum* on a fibroblasts-populated dermis (Fig. 1A). Twenty-four hours after exposure to UV_A and UV_B radiation, histological staining revealed the presence of classical sunburn cells detected in the suprabasal compartment of our reconstructed epidermis and a clear reduction of the neo-synthesis of extracellular matrix at the dermal level (Fig. 1B).

Systemic application of *Vitis Vinifera* before irradiations clearly protected the skin from these UV-induced damages (Fig. 1C).

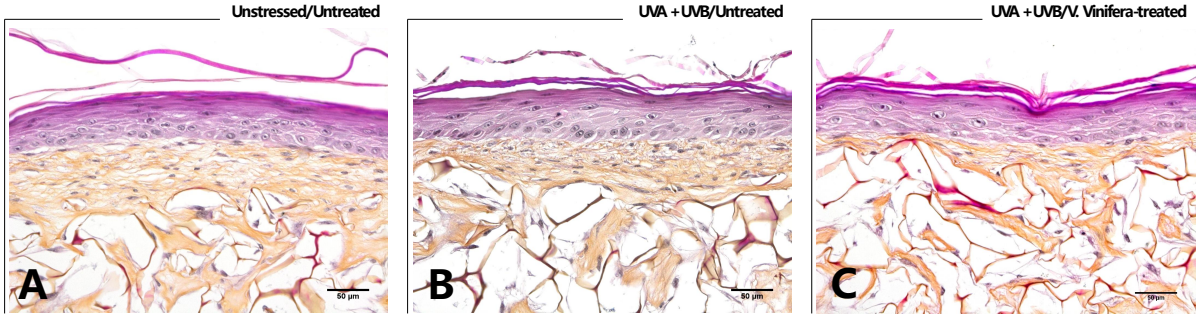

Fig. 1: Histological analysis of 3D full-thickness skin equivalent models unexposed to UV radiation and untreated (**A**), exposed to UVA+UVB radiations and untreated (**B**) and exposed to UVA+UVB radiations and treated with *Vitis vinifera* extract (**C**).

In the UVA/UVB-exposed 3D skin model, UV radiation strongly impacted extracellular matrix-related markers by inhibiting type I collagen expression by 38% (p=4.70E-8) and increasing MMP-1 expression by 433% (p=1.09E-5). *V. vinifera* extract preventive treatment significantly counteracted these damages by decreasing MMP-1 (75%, p=3.65E-5) and increasing type I collagen (20%, p=0.0054), compared with the untreated UVA/B-exposed condition (Fig. 2).

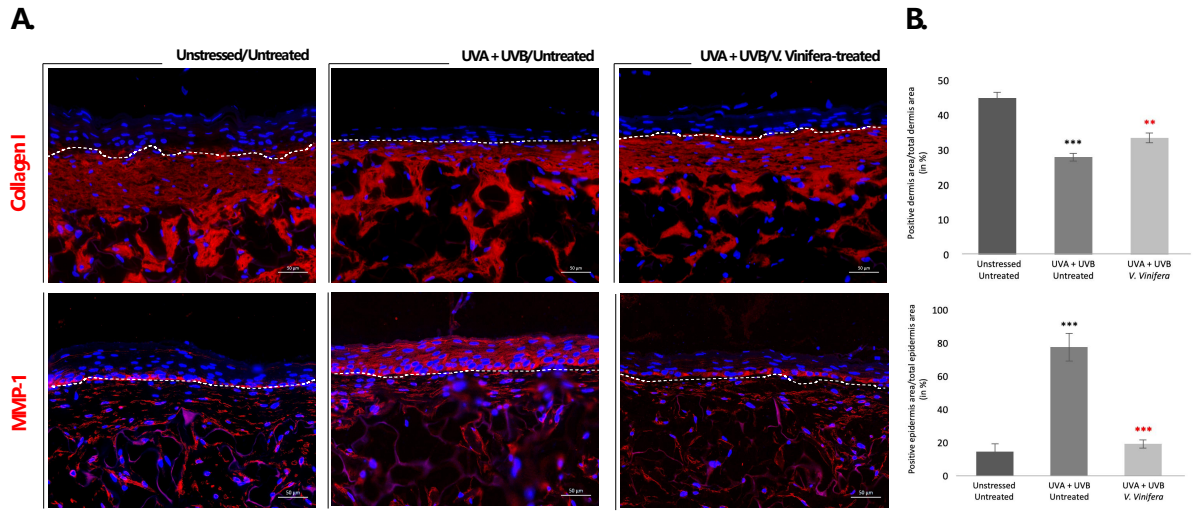

Fig. 2: Immunodetection (**A**) and image analysis (**B**) of extracellular matrix-related markers collagen I and MMP-1 expression in the 3D full-thickness skin equivalent models unexposed to UV radiation and untreated (left column), exposed to UVA+UVB radiations and untreated (middle column) and exposed to UVA+UVB radiations and treated with *Vitis vinifera* extract (middle column). Scale bar: 50 µm.

As shown in Fig. 3, oxidative stresses markers were also modulated by UV radiation in our 3D skin model. NQO1 and methallothionein were significantly increased by 166% (p=7.53E-10) and 387% (p=3.13E-9), respectively.

Treatment with *V. vinifera* extract reversed these deleterious effects by significantly decreasing NQO1 (72%, p=2.41E-10), and metallothionein (55%, p=1.79E-10).

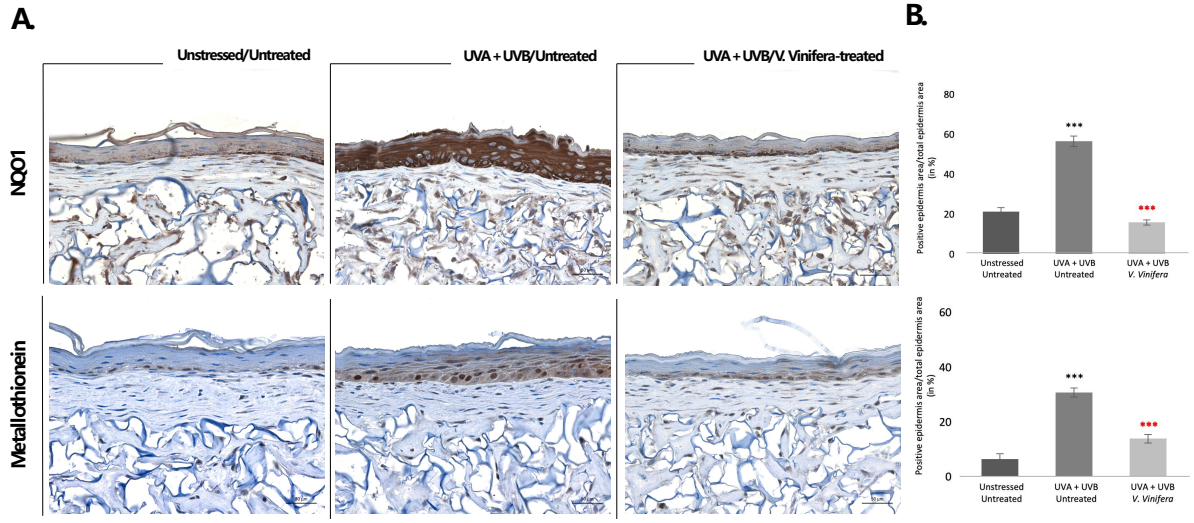

Fig. 3: Immunodetection (**A**) and image analysis (**B**) of oxidative stress markers NQO1 and metallothionein expression in the 3D full-thickness skin equivalent models unexposed to UV radiation and untreated (left column), exposed to UVA+UVB radiations and untreated (middle column) and exposed to UVA+UVB radiations and treated with *Vitis vinifera* extract (middle column). Scale bar: 50 µm.

Finally, UV radiations impacted epidermal differentiation and keratinocyte cohesion by significantly decreasing the expression of claudin-1, filaggrin, ceramides and LCE-1A by 53% (p=8.31E-9), 63% (p=4.58E-9), 93% (p=0.0002) and 97% (p=3.22E-6), respectively.

Systemic treatment with *Vitis vinifera* was able to prevent UV-induced epidermal alterations by significantly increasing claudin-1 by 80% (p=2.96E-5), filaggrin by 110% (p=0.0045), ceramides by 155% (p=0.0025) and LCE-1A by 1485% (p=0.0005), compared with untreated UV-exposed control condition.

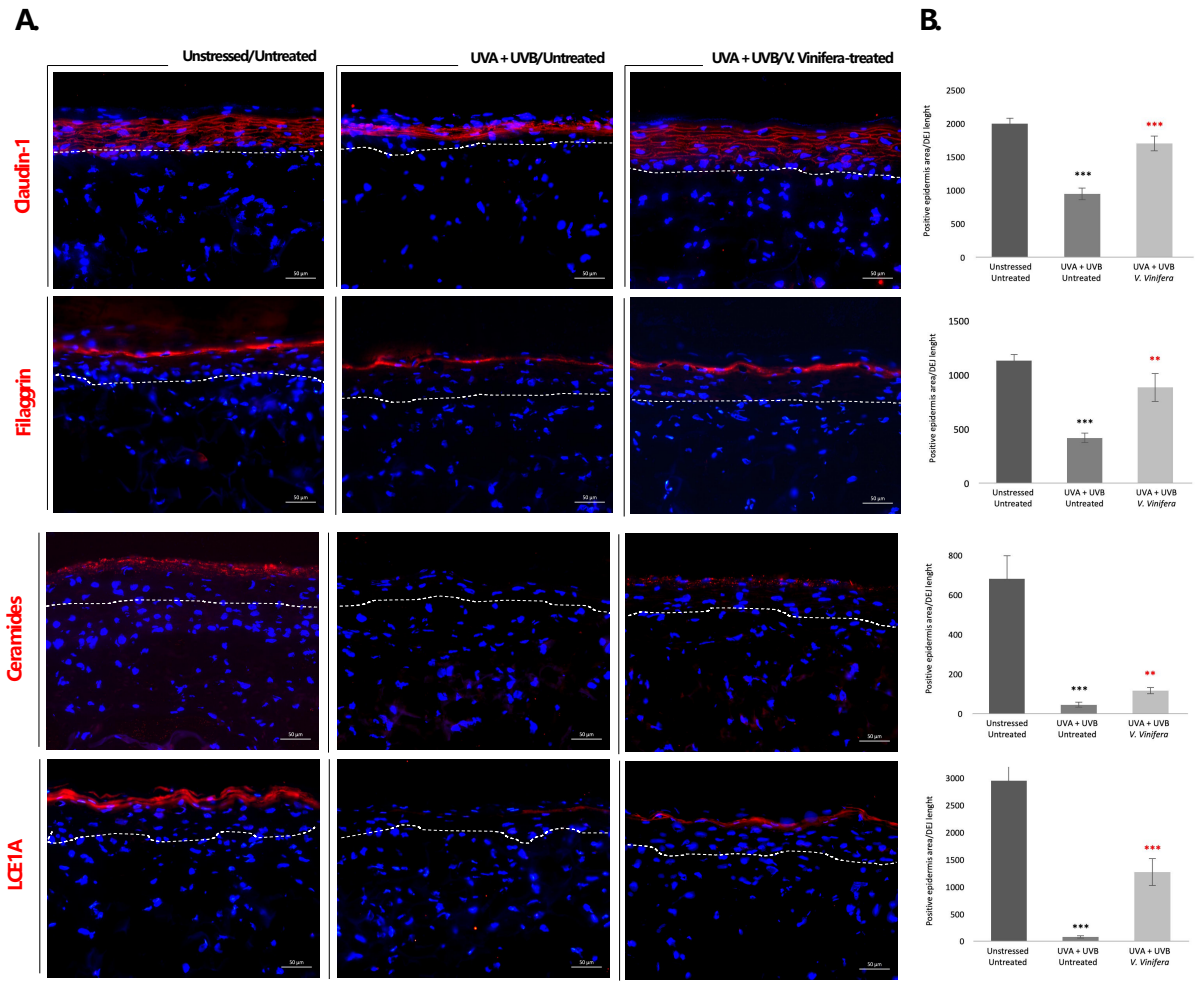

Fig. 4: Immunodetection (**A**) and image analysis (**B**) of epidermal-related markers claudin-1, filaggrin, ceramides and LCE1A expression in the 3D full-thickness skin equivalent models unexposed to UV radiation and untreated (left column), exposed to UVA+UVB radiations and untreated (middle column) and exposed to UVA+UVB radiations and treated with *Vitis vinifera* extract (middle column). Scale bar: 50 µm.

3.2 Vitis viniferas prevents pollution-related deleterious effects in a 3D full-thickness reconstructed model

To explore the efficiency of *Vitis Vinifera* extract in preventing skin against skin damage from environmental pollution, we first perfected a full-thickness 3D adult human skin equivalent exposed to urban dust. As can be seen in Fig. 5, histological analysis revealed that exposure to urban dust pollutant significantly disturbed the epidermal differentiation and extracellular matrix synthesis (Fig. 5B), compared with the unstressed control condition (Fig. 5A). Interestingly, exposure to *Vitis vinifera* clearly protected from pollutant damages with a well-developed and stratified epidermis and dense dermal equivalent (Fig. 5C).

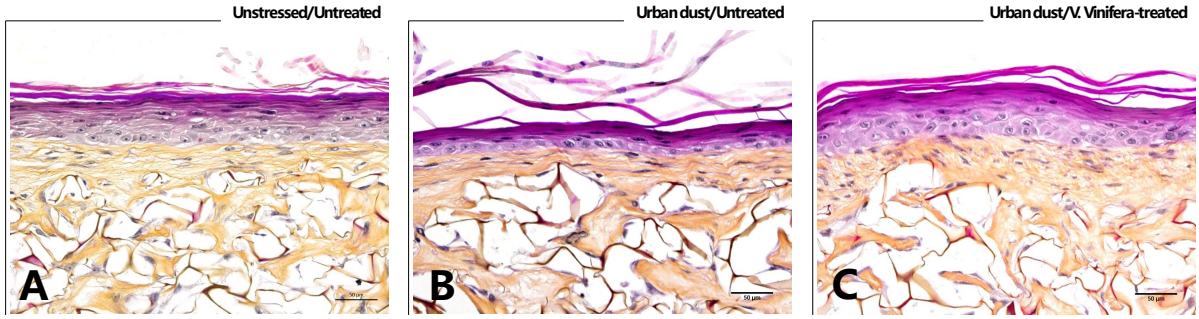

Fig. 5: Histological analysis of 3D full-thickness skin equivalent models unexposed to urban dust and untreated (**A**), exposed to urban dust and untreated (**B**) and exposed to urban dust and treated with *Vitis vinifera* extract (**C**).

In the urban dust-exposed 3D skin model, pollutants significantly impacted extracellular matrix-related markers by inhibiting type I collagen expression by 48% (p=1.45E-9) and increasing MMP-1 expression by 370% (p=0.0003). *V. vinifera* extract preventive treatment significantly counteracted these damages by inhibiting MMP-1 (62%, p=0.0024) and type I collagen (29%, p=0.0033), compared with the untreated urban dust-exposed condition (Fig. 6).

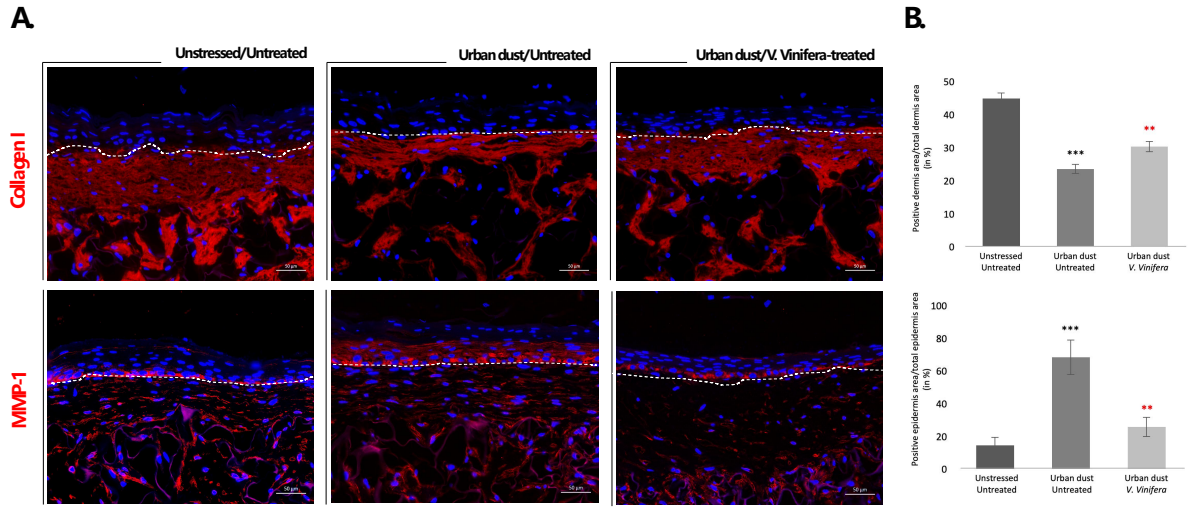

Fig. 6: Immunodetection (**A**) and image analysis (**B**) of extracellular matrix-related markers collagen I and MMP-1 expression in the 3D full-thickness skin equivalent models unexposed to urban dust and untreated (left column), exposed to urban dust and untreated (middle column) and exposed to urban dust and treated with *Vitis vinifera* extract (middle column). Scale bar: 50 µm.

As shown in Fig. 7, oxidative stresses markers were also modulated by urban dust exposure in our 3D skin model. NQO1 and methallothionein were significantly increased by 152% (p=1.49E-5) and 188% (p=0.0088), respectively.

Treatment with *V. vinifera* extract reversed these deleterious effects by decreasing NQO1 (77%, p=2.41E-10), and metallothionein (32%, p=0.23 – not significant).

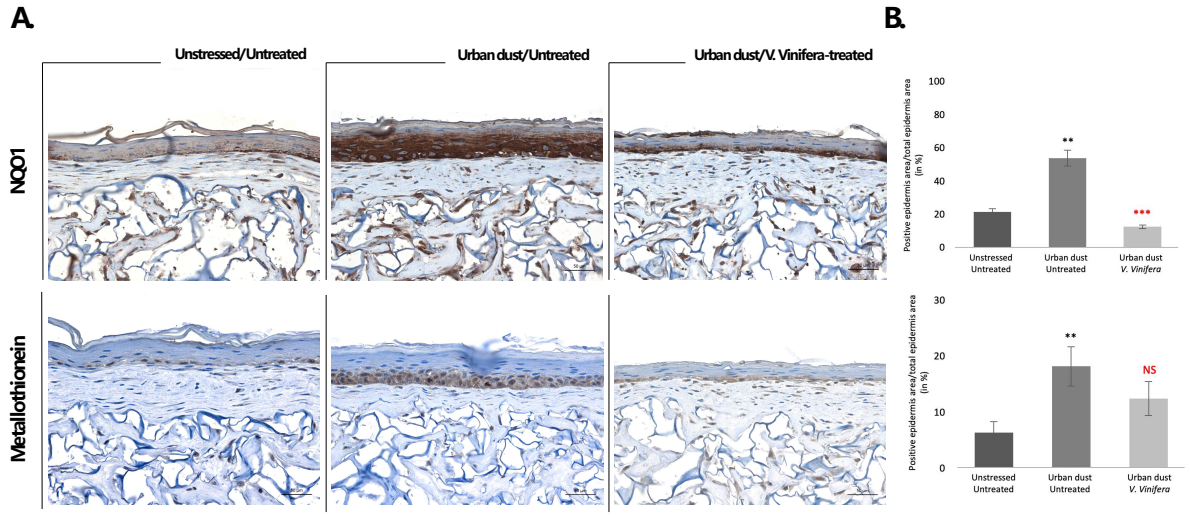

Fig. 7: Immunodetection (**A**) and image analysis (**B**) of oxidative stress markers NQO1 and metallothionein expression in the 3D full-thickness skin equivalent models unexposed to urban dust and untreated (left column), exposed to urban dust and untreated (middle column) and exposed to urban dust and treated with *Vitis vinifera* extract (middle column). Scale bar: 50 µm.

Finally, urban dust pollution impacted epidermal differentiation and keratinocyte cohesion by significantly decreasing the expression of claudin-1, filaggrin, ceramides and LCE-1A by 58% (p=2.89E-8), 61% (p=2.63E-9), 93% (p=0.0002) and 95% (p=3.30E-6), respectively.

Systemic treatment with *Vitis vinifera* was able to prevent urban dust-induced epidermal alterations by significantly increasing claudin-1 by 91% (p=1.84E-5), filaggrin by 120% (p=1.52E-6), ceramides by 38% (p=0.58 – not significant) and LCE-1A by 1884% (p=1.71E-6), compared with untreated urban dust-exposed control condition.

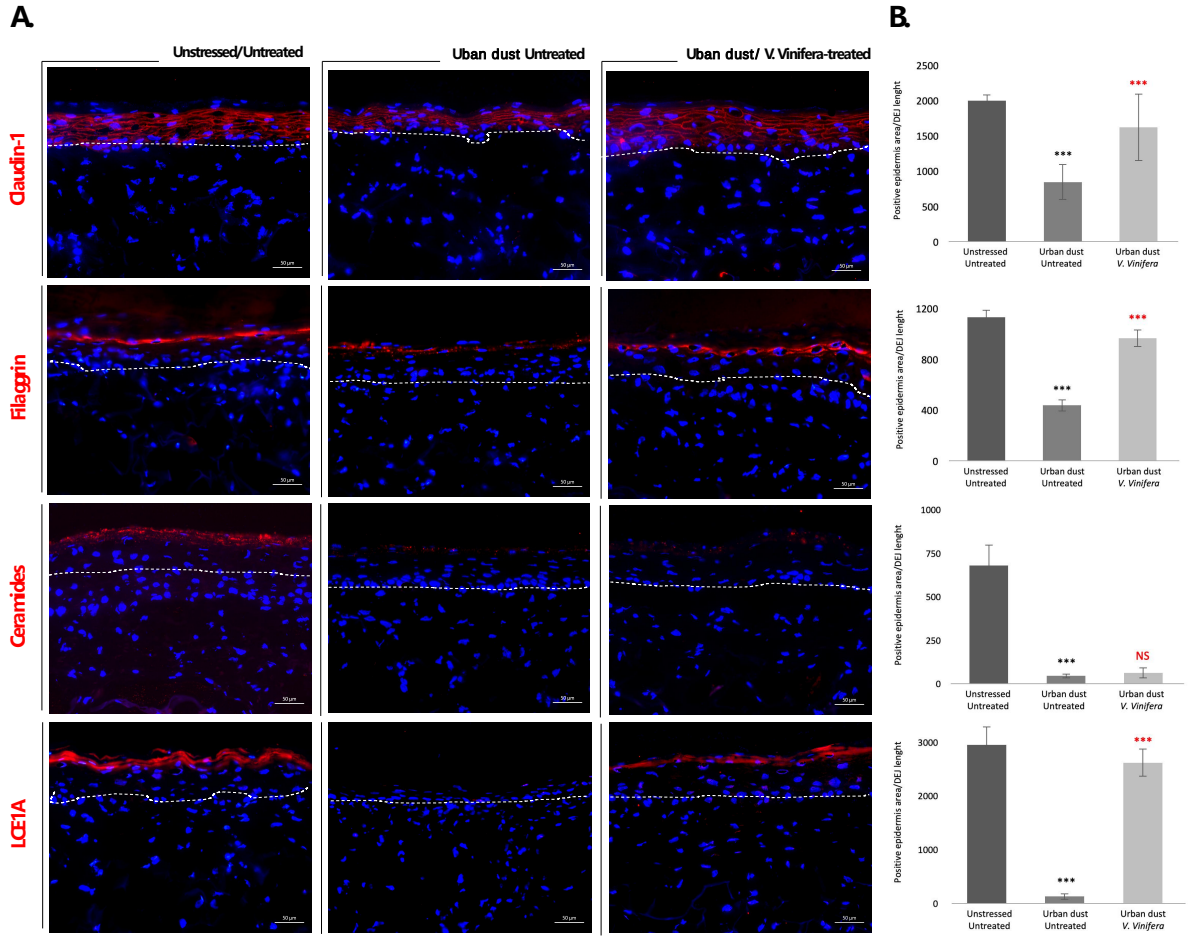

Fig. 8: Immunodetection (**A**) and image analysis (**B**) of epidermal-related markers claudin-1, filaggrin, ceramides and LCE1A expression in the 3D full-thickness skin equivalent models unexposed to urban dust and untreated (left column), exposed to urban dust and untreated (middle column) and urban dust and treated with *Vitis vinifera* extract (middle column). Scale bar: 50 µm.

3.3 Vitis Viniferas counteracts SDS detrimental damages in a 3D full-thickness reconstructed model

To assess the efficiency of *Vitis Vinifera* extract in protecting skin against irritation, we developed a full-thickness 3D adult human skin equivalent exposed to SDS solution. Compared to the unstressed condition (Fig. 9A), histological analysis of the 3D skin reconstructed samples revealed an apparent impact of the SDS on the thickness of the epidermis and density of the dermal equivalent (Fig. 9B). Treatment with *Vitis vinifera* extract counteracts SDS detrimental damages at both epidermal and dermal levels (Fig. 9C).

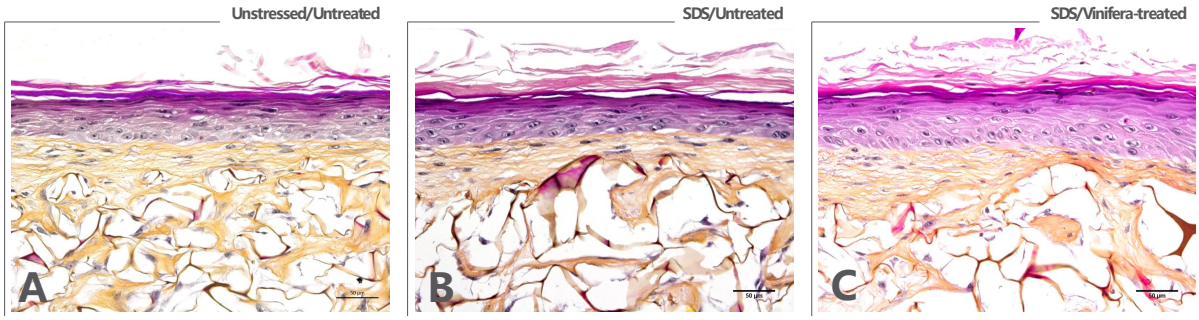

Fig. 9: Histological analysis of 3D full-thickness skin equivalent models unexposed to SDS and untreated (**A**), exposed to SDS and untreated (**B**) and exposed to SDS and treated with *Vitis vinifera* extract (**C**).

In the SDS-exposed 3D skin model, immuhistological analysis revealed a significant impact of this stress on the extracellular matrix-related markers by inhibiting type I collagen expression by 52% (p=6.12E-10) and increasing MMP-1 expression by 341% (p=3.59E-6). *V. vinifera* extract preventive treatment counteracted these damages by inhibiting MMP-1 (15%, p=0.27 -0 non sigificant) and type I collagen (52%, p=3.13E-5), compared with the untreated SDS-exposed condition (Fig. 10).

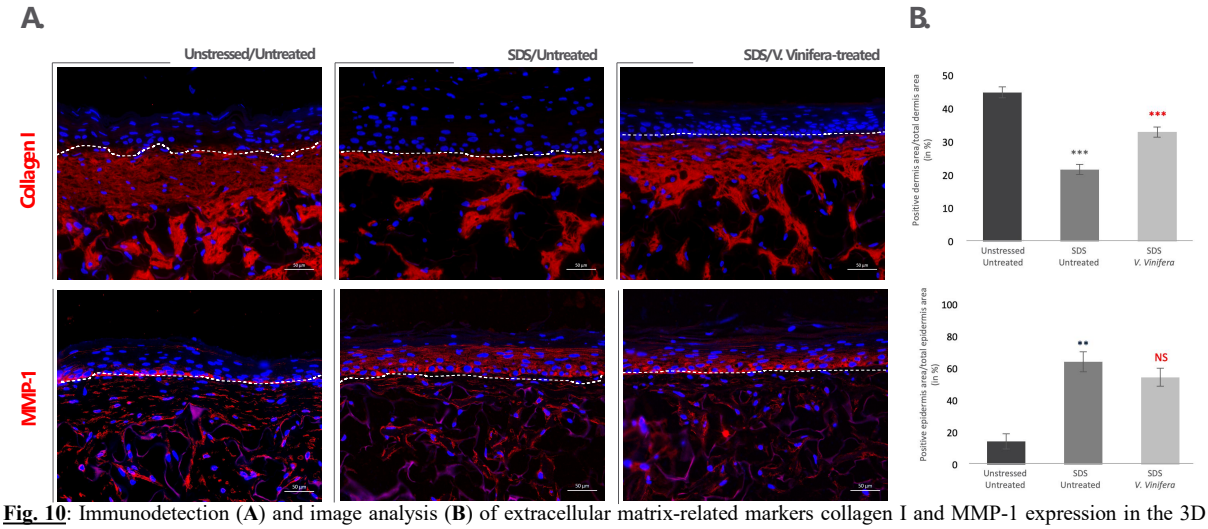

Fig. 10: Immunodetection (**A**) and image analysis (**B**) of extracellular matrix-related markers collagen I and MMP-1 expression in the 3D full-thickness skin equivalent models unexposed to SDS and untreated (left column), exposed to SDS and untreated (middle column) and exposed to SDS and treated with *Vitis vinifera* extract (middle column). Scale bar: 50 µm.

As shown in Fig. 11, oxidative stresses markers were also modulated by SDS exposure in our 3D skin model. NQO1 and methallothionein were significantly increased by 147% (p=1.67E-10) and 266% (p=2.91E-6), respectively.

Treatment with *V. vinifera* extract was only able to protect from these deleterious effects by decreasing NQO1 (10%, p=0.009), while metallothionein was not significantly modified.

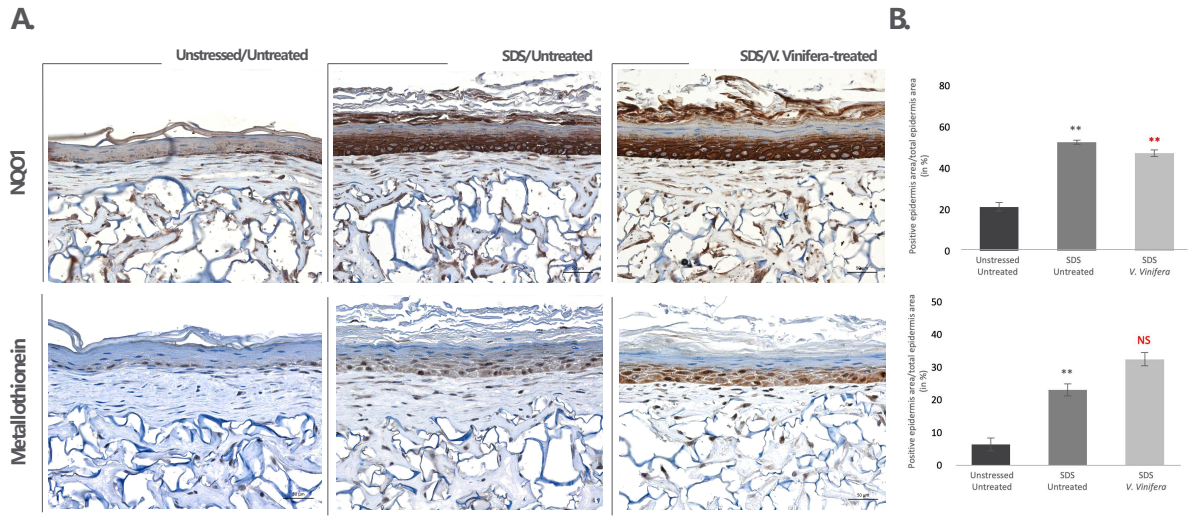

Fig. 11: Immunodetection (**A**) and image analysis (**B**) of oxidative stress markers NQO1 and metallothionein expression in the 3D full-thickness skin equivalent models unexposed to SDS and untreated (left column), exposed to SDS and untreated (middle column) and exposed to SDS and treated with *Vitis vinifera* extract (middle column). Scale bar: 50 µm.

SDS impacted epidermal differentiation and keratinocyte cohesion by significantly decreasing the expression of claudin-1, filaggrin, ceramides and LCE-1A by 42% (p=1.42E-7), 9% (p=0.38 – not significant), 95% (p=0.0002) and 86% (p=5.89E-6), respectively. Systemic treatment with *Vitis vinifera* at 0.1% was not able to prevent SDS deleterious impacts at the epidermal level (Fig. 12).

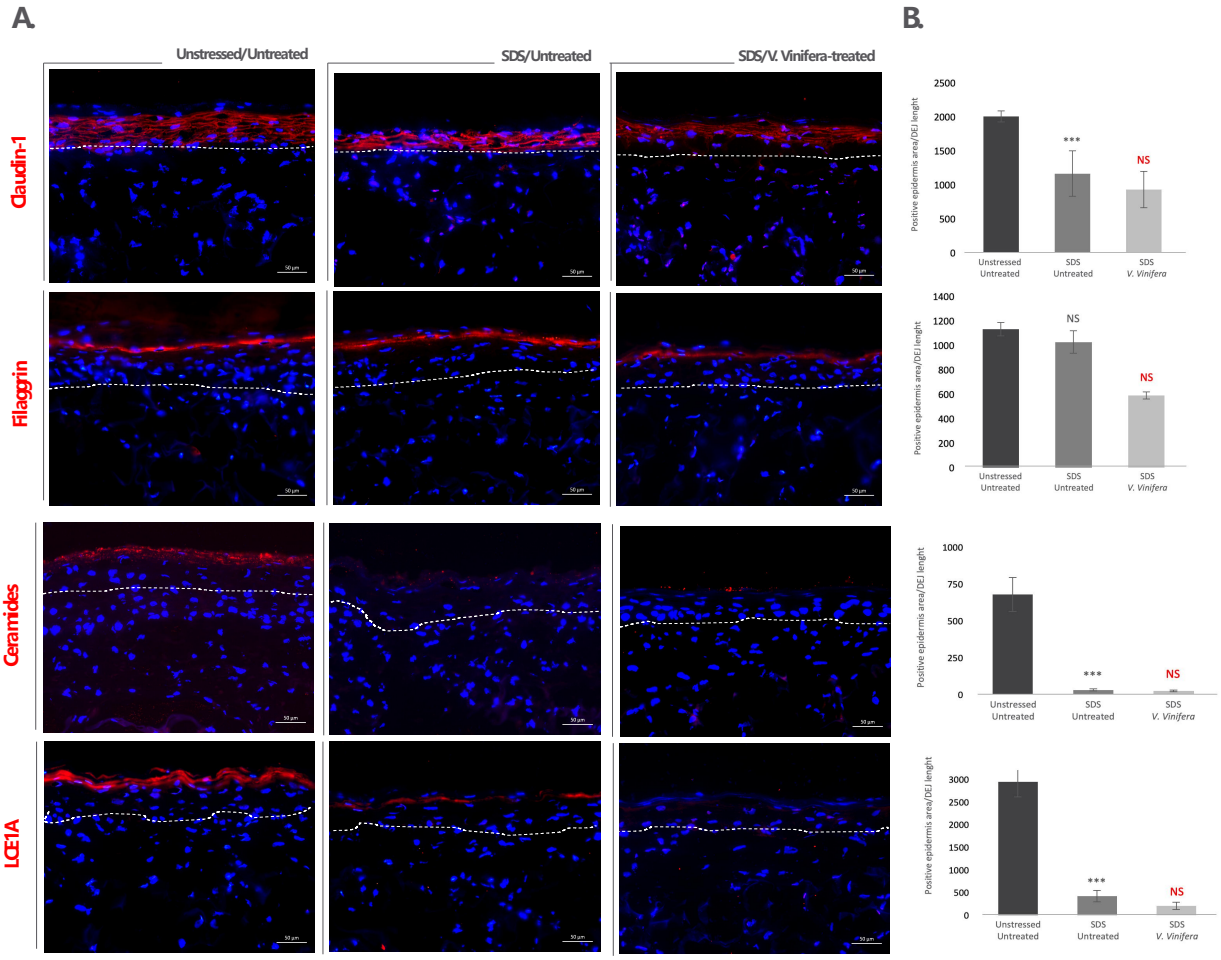

Fig. 12: Immunodetection (**A**) and image analysis (**B**) of epidermal-related markers claudin-1, filaggrin, ceramides and LCE1A expression in the 3D full-thickness skin equivalent models unexposed to SDS and untreated (left column), exposed to SDS and untreated (middle column) and SDS and treated with *Vitis vinifera* extract (middle column). Scale bar: 50 µm.

4. Conclusion

Overall, the present in vitro study demonstrated that application of *V. vinifera* extract on a 3D full-thickness human skin model exposed to different environmental aggressions prevented upregulation of oxidative markers by inhibiting NQO1 and metallothionein, improved skin barrier function by up-regulating filaggrin, LCE-1A, claudin-1 expression and also by stimulating extracellular matrix-related proteins such as type I collagen.

In conclusion, application of V. vinifera significantly counteracts the effects of exposome aggressions in an *in vitro* skin model, suggesting its protective effects against daily UV and pollutant exposure.

5. Acknowledgments

We would like to express our sincere gratitude to Gangzhou Jiyan Cosmetics Technology Co., Ltd. for providing experimental materials and financial assistance, as well as Ms. Li Hui and Mr. Song Ximing from Gangzhou BIKE Biotechnology Co., Ltd. for providing translation and consulting services.

6.Conflict of Interest Statement.

NONE

References.

[1] Concepcion Parrado, Sivia Mercado-Saenz, Azahara Perez-Davo, Yolanda Gilaberte et *al*. Environmental Stressors on Skin Aging. Mechanistic Insights. Front Pharmacol. 2019; 10: 759.

[2] Jennifer Salsberg, Anneke Andriessen, Sonya Abdulla, Renita Ahluwalia et *al*. A review of protection against exposome factors impacting facial skin barrier function with 89% mineralizing thermal water. J Cosmet Dermatol. 2019 Jun;18(3):815-820.

[3] Monika Michalak. Plant-Derived Antioxidants: Significance in Skin Health and the Ageing Process. Int J Mol Sci. 2022 Jan; 23(2): 585.

[4] Tarfah Al-Warhi, Eman Maher Zahran, Samy Selim, Mohammad M. Al-Sanea, et al. Antioxidant and Wound Healing Potential of Vitis vinifera Seeds Supported by Phytochemical Characterization and Docking Studies. Antioxidants (Basel). 2022 May; 11(5): 881.

[5] Germain L, Rouabhia M, Guignard R, Carrier L, Bouvard V, Auger FA. Improvement of human keratinocyte isolation and culture using thermolysin. Burns J Int Soc Burn Injuries. 1993;19:99–104.

[6] Morgan Dos Santos, Elodie Metral, Aurélie Boher, Patricia Rousselle et al. In vitro 3-D model based on extending time of culture for studying chronological epidermis aging. Matrix Biol. 2015 Sep;47:85-97.